

OPTIMALISATION OF MPEG LENGTH AND MPEG/DNA DENSITIES FOR AUNP FUNCTIONALIZATION

BACHELOR THESIS IN BIOMEDICAL TECHNOLOGY

Stijn Wiggerts

November, 2023

Examination committee

Prof. Dr. Ir. L.I. Segerink

Prof. Dr. A. Kocer

Dr. Ir. J.E. van Dongen

Department

BIOS - Biomedical and Environmental Sensorsystems

Faculty

EEMCS

UNIVERSITY
OF TWENTE.



Contents

1	ABSTRACT	4
2	SAMENVATTING	4
3	INTRODUCTION	5
4	THEORETICAL FRAMEWORK	6
4.1	Light altering properties of AuNPs	6
4.2	ssDNA detection	6
4.3	AuNP functionalization	7
4.4	Gold nanoparticle stability	8
5	MATERIALS & METHODS	11
5.1	Fluorescent DNA calibration	11
5.2	functionalised AuNPs	12
5.3	Gold nanoparticle calibration by absorbance	12
5.4	DNA density and mPEG chain length	13
5.5	ssDNA binding to HS-DNA on AuNPs	14
6	RESULTS AND DISCUSSION	16
6.1	Fluorescence calibration	16
6.2	AuNP stability when coated with mPEG and tween20	17
6.3	Gold nanoparticle calibration curve	20
6.4	Optimal HS-DNA loading on AuNPs	22
6.5	Optimal target DNA loading	25
7	CONCLUSION	28
8	OUTLOOK	29
8.1	Future research	29
8.2	implications	29
9	ACKNOWLEDGEMENTS	30
10	APPENDIX	34
10.1	Original protocol	34
10.2	Fluorescent DNA calibration	35
10.3	Limit of detection for fluorescence	36
10.3.1	Comparison between fluorescence with and without MCE	37
10.4	Gold nanoparticle stability	37
10.5	Gold nanoparticle dilution series	38
10.6	HS-DNA loading on AuNPs	41

10.7 target DNA loading	42
10.7.1 washing steps calculation	42
10.7.2 Fluorescence comparison, target DNA, unbound target DNA and blancos . .	43
10.8 additional information	43

1 ABSTRACT

Cancer remains one of the most common causes of death worldwide. Treatment is often possible but the chance of survival decreases with increasing tumour size. As such early detection is crucial for a high survival rate. Currently we are lacking a specific, place of care, risk free, detection. Mutated DNA is a specific biomarker that can be used for cancer detection. Using the protocol adapted from Li et al.¹ HS-DNA can be conjugated to gold nanoparticles. With this process complementary, mutated, DNA can bind indirectly to two AuNPs. This brings multiple particles closer together, eliciting a colour change, thus allowing mutated DNA to be detected.

This thesis aimed to maximise the number of target DNA strands bound per AuNP to increase detection sensitivity. Fluorescent HS-DNA was conjugated to AuNPs coated with different surface molecules. AuNP concentration was measured using absorbance, while HS-DNA concentration was measured using fluorescence. The results showed larger surface molecules have a positive effect on direct DNA conjugation to the particles. Additionally, this thesis has shown optimizations in methods for functionalizing AuNPs. Target DNA loading was also measured. However, target DNA did not show any increase across different HS-DNA loading or surface molecules. More research is needed to find an optimum for target DNA binding.

2 SAMENVATTING

Kanker is een van de meest voorkomende doodsoorzaken. Behandeling is vaak mogelijk, maar de overlevingskans neemt af voor grotere tumoren. Het is dus cruciaal om tumoren zo vroeg te detecteren. Er zijn verschillende detectiemethoden, maar er mist nog een methode die gevoelig is, bij place of care diagnostiek gebruikt kan worden en die geen patientrisico oplevert. Omdat tumorcellen gemuteerde cellen zijn, is gemuteerd DNA een goede biomarker voor kanker. Li et al.¹ hebben een protocol waarmee men HS-DNA aan goud nanodeeltjes (AuNPs) kan conjugeren. Het gemuteerde DNA kan binden aan het HS-DNA, en dus indirect aan de goudnanodeeltjes. Zolang het juiste HS-DNA wordt gekozen kan het gemuteerde DNA (Target DNA) binden en zo de AuNPs bij elkaar brengen. Dat zorgt voor een kleurverandering in het goud waardoor het DNA optisch gedetecteerd kan worden.

In dit verslag is geprobeerd om target DNA binding per AuNP te optimaliseren. De hoeveelheid AuNPs is gemeten met absorptie. DNA is gemeten door gebruik van fluorescente markers. De resultaten toonden aan dat er meer HS-DNA binding is wanneer de AuNPs ook met grotere oppervlakte moleculen worden bedekt. Verder zijn er optimalisaties aangetoond in de methode voor DNA conjugatie. Target DNA is ook gemeten. Er is geen verschil in target DNA binding gevonden bij verschillende oppervlakte moleculen en/of verschillende HS-DNA concentraties. Hier is meer onderzoek voor nodig.

3 INTRODUCTION

Cancer is one of the leading causes of death in the modern world, with 10 million deaths estimated worldwide in 2020.² While techniques for fighting cancer are advancing fast, early detection remains crucial to ensure a high survival rate.

Current methods for detecting cancer include x-rays, Magnetic resonance imaging (MRI), positron emission tomography (PET) and optical methods. While these are accurate at detecting relatively large tumours, they have their drawbacks. For example, PET scans and x-rays subject the patient to a dose of radiations, Optical methods need surgical intervention if the suspected tumour is on the inside of the body, and all these methods are time intensive and costly.³ There are non invasive methods based on the detection of biomarkers like hormones, but these lack often sensitivity. Also, due to the fluctuating nature of some biomarkers, there is a possibility for edge cases to go unnoticed.^{3,4}

Detecting DNA is a good alternative to find early stage tumors with high certainty. Techniques to detect DNA in order to diagnose cancer already exist.⁴ However, there are problems with the current gold standards. Methods like qPCR require complex setups, time, skilled labour, and often require extra steps to acquire a clear result.⁵ The drawbacks of common methods facilitated the need to create a new, easy to use, sensitive and specific way to detect DNA.

The field of DNA detection can be brought forward with gold nanoparticles (AuNPs). Detecting DNA by conjugating complementary strands to AuNPs shows to be sensitive enough to detect DNA in the pico- to femtomolar range.^{6,7} Its working principle lies with the specific surface properties of AuNPs: high localised surface plasmon resonance (LSPR). This optical property allows AuNPs to be detected using visible light.

Furthermore, the specific plasmon resonance is dependent on both size and shape of the AuNPs.⁸ Moreover, the LSPR is distance dependent. When two or more AuNPs get close, the surface plasmons couple.^{7,9} This coupling changes the way the electrons interact with passing photons. This colour change means the AuNPs visibly change colour when brought close together.^{6,7,10,11}

Different techniques exist for detecting cancer using AuNPs.¹² There are many protocols for conjugating DNA to the surface of the AuNPs. Unfortunately, there is no gold standard. Many protocols have inefficiencies or take multiple days to set up.^{6,12} This thesis will take the protocol of li et al (Oct 2014),¹ as it has proven to be relatively fast and effective. The goal is to optimise this protocol. "Optimal" is defined as being able to bind as much ssDNA per AuNP as possible. More ssDNA binding to each AuNP corresponds to a higher likelihood of 2 AuNPs binding to the same molecule. This corresponds to a lower detection limit and a higher signal at the same target DNA concentration. This way AuNPs optimization corresponds to a more sensitive cancer detection method.

In short, the focus of this thesis is to optimise an existing protocol in order to detect the maximum number of ssDNA strands per AuNP. First, this thesis will treat the underlying theory of DNA detection using AuNPs. Following on the theory, the different experimental setups will be described, followed by a discussion of the individual results. At the end of the thesis a general conclusion will be drawn and possible implications will be covered.

4 THEORETICAL FRAMEWORK

In this framework the functionality of AuNPs will be discussed, as well as the modifications done to the AuNPs to use them for (hypermethylated¹³) DNA detection.

4.1 Light altering properties of AuNPs

As stated, AuNPs experience LSPR. In this section LSPR will be outlined. When photons pass a metal surface, Electrons on the surface can start moving synchronised to the photons.¹⁴ The small size of AuNPs hinders plasmon movement in the direction of the photons, hence the name "Localised Surface Plasmon Resonance".^{14,15} This resonance can cause interactions with wavelengths that are larger than the particles. This effect makes individual gold nanoparticles visible when using dark field microscopy, even when the particles are smaller than the wavelengths in visible light¹³

The AuNPs used in this thesis do not spontaneously coagulate, generally, the colloid consist of independent particles. This is because citrate capped particles are stabilised by their negative surface charge.¹ Even though the particles generally stay apart, we can chemically and physically force the AuNPs to stay in close proximity with each other by binding molecules to their surface.

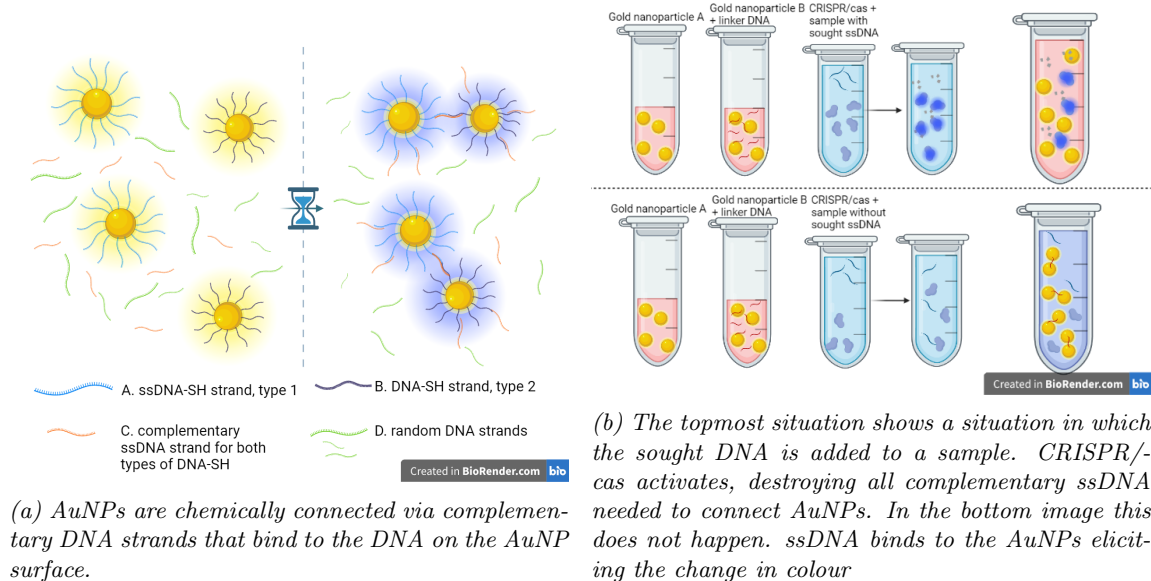
Scattering due to LSPR is both dependant on the size and the distance between the AuNPs. When two or more particles come into close proximity with each other, electrons can move between the particles with relative ease; The plasmons start to interact and their light scattering behaviour becomes more akin to that of a single, larger, particle.¹⁶

By forcing the AuNPs in close proximity with the use of surface molecules, we can optically detect if these molecules are present. The surface molecules used in this bachelor assignment are HS-DNA strands. These strands can be tuned to be complementary to the DNA we want to detect, the target DNA. Being complementary, they will bind to the target DNA. If two HS-DNA strand (with the AuNP attached) bind to the two ends of a target DNA strand, the AuNPs are forced to stay close together. Using this method target DNA can be detected optically. This is explained more in depth in the following section.

4.2 ssDNA detection

There are two ways in which AuNPs can be used to detect DNA. With the first method AuNPs get functionalised with different kinds of DNA. When an added sample contains the complementary ssDNA strand it will link two AuNPs, eliciting the colour change. This change is specific to just a few coupled AuNPs, so dark field microscopy can be used to detect if there is complementary DNA.¹³ This process is illustrated in figure 1a. A variation on this process utilises AuNPs bound to a (gold)substrate with "hairpin" DNA, as is described in van Dongen.¹³

The second method is much the same as the first, however, a specific CRISPR/cas protein is also added. CRISPR/cas can be tuned to activate when it comes into contact with targeted DNA strands. When CRISPR/cas detects this DNA it gets activated to cut all ssDNA strands, including the linker strands. With no functional linker DNA remaining the AuNPs cannot bind and the colour change will not take place.^{7,13,17} In this way either zero or all strands will be destroyed. The effect of this is a radical colour change, as is shown in figure 1b.¹⁷



4.3 AuNP functionalization

Both techniques described in the previous section require the AuNPs to be functionalised with added DNA strands. This proves difficult because only mild conditions can be used; After all, the DNA strands must remain intact. Furthermore, citrate capped AuNPs have a negative surface charge which stabilises the particles. Unfortunately it also hinders DNA binding because DNA is also negatively charged.¹ The issue with this is that AuNPs and DNA stay too far apart for reactions to take place. A solution is adding salt to the mixture. The ions can mitigate the charge of DNA.^{1,19}

Due to the salt addition, the electrostatic repelling forces keeping the AuNPs stable will also be screened. As such the AuNPs will coagulate when salt is added.¹⁰ A workaround is to first cover the AuNPs with molecules, so they cannot coagulate due to steric effect. The molecules used to cover the AuNPs are tween20 and thiolated methoxy polyethylene glycol. (mPEG-SH, but in this thesis often shortened to mPEG) Both molecules can interact with gold and when added in excess enough molecules bind to sterically prevent coagulation.

Both mPEG and tween20 can bind, so why would one type of molecule not be enough? The answer lies with the different bindings. the mPEG is made to bind by the addition of a thiol group.²⁰ Because the DNA molecules are modified the same way both DNA and mPEG will form very similar

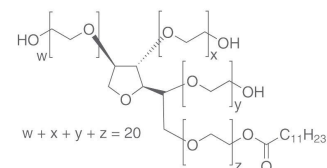


Figure 2: The structure of tween20. Notice tween20 is a group of isomers with an identical anchor group and variable length "arms".¹⁸

strength bonds. However, the bond between tween20 and DNA is weaker since tween20 only adheres because it is a surfactant in an aqueous solution. This is nicely illustrated by its molecular structure (see figure 2). The effect of this weak bond is that DNA can bind more easily to the AuNPs by taking the place of tween20 molecules.

The procedure is now as follows: First the surface molecules (tween20 & mPEG) are added to an aqueous solution of AuNPs. Next both salt and the DNA are added. During incubation the DNA will replace the tween20 molecules, so the AuNPs are functionalised. However, there are many molecules of tween20, mPEG, salt and DNA that are not bound. In order to remove these the solution can be centrifuged and washed. After washing, the particles are functionalised. In this thesis, the protocol will be optimised.

4.4 Gold nanoparticle stability

In order to find the optimal protocol, there are some constraints. One of these constraints is that the AuNPs must remain stable. Coagulated AuNPs cannot be brought closer together by DNA binding, and as such are of no use. Subsection 4.3 illustrates why mPEG is necessary. However, the addition of mPEG can have some consequences on DNA loading. To prevent failed and/or unnecessary experiments, the minimal and maximal mPEG loading needs to be determined, while keeping in mind the necessary addition of tween20.

First, the surface area of the AuNPs needs to be determined per volume. In order to do this, the stock AuNP concentration was calculated using the Beer-Lambert law as described in the section above. Based on the concentration and the particle diameter, the surface area per particle can be calculated using equation 2, assuming all particles are perfectly spherical.

$$A = 4\pi r^2 \tag{1}$$

Although the particles are not perfect, for 40 nm particles this assumption is reasonable based on the average size and size deviation statistics provided for the AuNPs. According to the supplier the particles are between 37.0 and 43.0 nm, with at most 5% having odd shapes.²¹

By using the concentration found with the absorbance, the number of particles per volume can be calculated. By multiplying the number of particles with the surface area per particle the total surface area per volume can be found. This comes down to $2,36E+14$ nm²/ml for particles of 40 nm. This value will be used when calculating the minimal mPEG concentration needed to reach full coverage. How do we know what density corresponds to "full coverage"?

For mPEG both density and chain length affect coverage. Based on the loading density, and the chain length the mPEG chains can take up two conformations. These conformations affect the how much of the AuNP is sterically protected from coagulating. There is the shorter, more entwined, mushroom conformation and the longer, more linear, brush conformation. (This can be seen in figure 3) The conformation of the surface molecules influences many AuNP properties.²²⁻²⁴ The assumption is made that when the brush conformation is adopted, the AuNPs are covered such that they cannot coagulate anymore. After all, in brush conformation the molecules are fully stretched out, leading to the chains taking up space further away from the particle surface than in mushroom conformation.

In order to find when a certain conformation is reached the Flory radius can be used.^{25,26} The Flory radius is expressed as:

$$R_f = \alpha N^s \quad (2)$$

This equation uses the number of repeat units N to express the chain length. The exponent is determined by the solvent and is about 0.6 in water.²⁶ The length of each monomer corresponds to the parameter α . Since both the molecular weight of the chains and the structure of mPEG are known, the number of monomers can be calculated.²⁶

When the distance between chains is smaller than the Flory radius, the chains adopt a brush conformation. The Flory radius for 6kDa mPEG is calculated to be 6,68 nm. For 2 kDa it is 3,45 nm and for 0.8 kDa mPEG it is 1,99 nm. If the same concentration of mPEG is to be used with different chain lengths, the lower bound is dependent on the shortest mPEG chains used. Due to a problem with acquiring 0.8 kDa mPEG, the smallest molecule that will be used is 2 kDa mPEG. The highest possible density is also known. The highest density found for 6 kDa mPEG is lower than 4,7 strands/nm².²² since longer chains have a lower maximum loading density (attributed to more steric effect). The maximal loading density has been assumed to be between the 4,7 chains/nm². It is not known with what

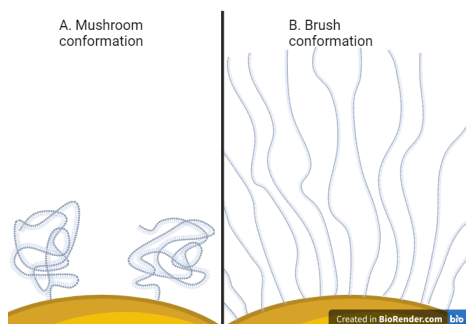


Figure 3: A 2d graphic representation of the two possible conformations. The mushroom conformation is a random conformation, which changes based on the binding energy. For brush conformation, the steric effect hinders the random walk. For curved surfaces, the particles can take a partial brush and a partial mushroom conformation.²⁷

efficiency the binding takes place, which is why this experiment will be carried out with a range of added concentrations. The protocol is illustrated in chapter 5.2.

Using the radius of 3,45 nm for 2kDa mPEG, the loading density can be calculated. The Flory radius can be used to calculate the surface area of that is "protected" by the chain. We can use the total surface area of an average AuNP to calculate the amount of AuNPs needed per particle. For 40 nm AuNPs and 2kDa mPEG this will come down to:

$$\frac{5,03 * 10^3}{2 * \pi * 3,45^2} = 67.25 \text{chains/NP}. \quad (3)$$

But this formula assumes the surface area of all chains perfectly covers the entire surface of the AuNP. This is not the case. The Flory radius does not coincide with the maximal loading of particles. The calculations above show the minimal number of chains needed to coat the particle, assuming each chain is placed perfectly. In reality, the molecules are placed randomly, so in some places they will be closer together than the maximal distance needed for the brush conformation. These imperfections increase the number of chains per AuNP needed to reach full brush conformation. For this experiment the researchers assumed random placement increases the number of mPEG strands needed by 20 %

Furthermore, we cannot assume the surface to be flat. The gold nanoparticles are (approximately) spheres. According to H.Hill et al.²⁷ for particles smaller than 60 nm across, the geometry has a influence on the behaviour of chain like particles. (although they only focused on DNA, a larger and more rigid molecule per monomer unit than mPEG) To combat this, the value is increased by another 47 %. This value is derived by calculating the difference in loading per surface area for 40 nm AuNPs versus a flat surface in the research done by H.Hill et al. This ends up at: 118.6 chains per AuNP, or a density of 0.0236 chains per nm².²⁷ The corresponding concentration added to stock AuNP solution is calculated to be 0.0185 μ M, assuming all mPEG molecules bind to the AuNPs. Which, in all likelihood, will not be the case.

5 MATERIALS & METHODS

5.1 Fluorescent DNA calibration

The first experiment was executed to create a calibration curve, relating known fluorophore concentrations to a measured fluorescence intensity, however, its function was twofold. It also served to determine the limit of detection of the instruments. As described in the sections above, AuNP functionalisation is inefficient; After functionalising AuNPs with DNA, there are many DNA molecules left over in the solution. DNA can interfere with the measurements. especially the fluorescent DNA strands form a strong confounding factor as they will be detectable in the wells even though they did not attach to the AuNPs. As such, it is important that all unbound DNA is removed. In order to remove DNA normally the sample will be washed, diluting the loose fluorophore concentration.

First, a calibration curve was made for fluorescent DNA. The DNA used was HS-polyA5-CiHSR35nt with the fluorophore atto 647n attached. (Eurofins, Leiden, the Netherlands) The DNA was diluted in phosphate buffered saline (PBS, Sigma-aldrich, Burlington, Massachusetts, United States)) DNA concentrations between 5 μM and 0,8 nM were tested.

Different sources state a different maximal DNA loading for 40 nm particles.²⁷⁻²⁹ Corresponding to the maximal loading, needed DNA and added DNA concentrations can be calculated. In contrast to this approach DNA is often added in a 10 to 100 fold excess, because DNA binding happens via an equilibrium reaction.^{28,29} So, in order to ensure compatibility with the original protocol, 5 μM is chosen as a maximal concentration. In the worst case, no DNA will bind to the AuNPs. As such, 5 μM is the maximal DNA concentration that needs to be diluted to below the L.O.D. It is not known what the detection limit is for the used fluorophore, which is why a dilution series with a wide range of concentrations will be made for a647n.

The dilution series can be seen in tables 1 through 4 in the appendix. In each step and series enough volume was pipetted to create a triplicate. A negative control was added consisting of PBS. for each condition 100 μl was added to a 96 well plate.

A second experiment was also done using a very similar setup, safe for two changes. First, the DNA was diluted in PBS with 0.01 %wt tween20 added. (Sigma-aldrich, Burlington, Massachusetts, United States) After creating the dilution series, 1,4 μl 2-Mercaptoethanol (Sigma-aldrich, Burlington, Massachusetts, United States) was added to each ml. This was done to find if the addition of 2-mercaptoethanol (MCE) changes fluorescence significantly. The tables 3 and 4 show this dilution series. Note the first part of the dilution series is identical to the experimental setup without added MCE.

After creating the dilutions, the fluorescence intensity was measured on the spectramax id5 microplate reader (Molecular devices, San Jose, USA). To find fluorescence, the wells were excited at 640 nm and emission was measured at 680 nm. The data was analysed to find a possible limit of detection. Additionally, a linear fit was created for the fluorescence (arbitrary units) and concentration (μM) to create the calibration curve.

5.2 functionalised AuNPs

The second experiment was done to determine the minimal needed mPEG concentration needed to stabilise the AuNPs. AuNPs are known to coagulate under high ionic strength conditions.³⁰ To ensure stability at the NaCl concentration needed for this experiment, the minimal needed mPEG coverage for this batch of AuNPs has been calculated. Based on this minimum the protocol has been set up.

The following protocol was carried out. To 100 μ L 40 nm AuNPs (BBI solutions, Crumlin, United kingdom) 1 μ L PBST was added. Next, mPEG was added to create different conditions. Each condition has a different mPEG concentration, ranging from 0,01 to 9 μ M. This can also be seen in table 5 in the appendix. Note the concentrations as stated the table have a deviation of 1 % because of the addition of PBST. Last MilliQ (made using the Milli-Q EQ 7008/16, Sigma-aldrich, Burlington, Massachusetts, United States) was added to equalize volume between tubes. After mixing and vortexing the tubes were incubated for 20 minutes, after which the salt concentration was increased to 1,16 M. The tubes were vortexed and pictures were taken after incubating for one hour.

Another experiment was done without adding tween20. For this experiment first 100 μ l AuNPs was added to the eppendorf tubes, after which the same mPEG concentrations and MilliQ was added as shown in table 5. The tubes were incubated for 20 minutes after which 50 μ l, 4M NaCl was added. The pictures, again taken after 1 hour of incubation, are discussed in chapter 6.2.

5.3 Gold nanoparticle calibration by absorbance

The follow-up experiments need to be precise. That is why it is important to accurately know the amounts of all different components in a medium. One of these components are the AuNPs. However, the AuNP concentration is not known. To determine an accurate reading of the AuNP concentration by absorption, a calibration curve needs to be made. First, the stock concentrations can be determined using the Beer-Lambert law.

$$A = \epsilon bC \quad (4)$$

A, absorbance is found using the nanodrop system.(Nanodrop 2000C, eppendorf, Nijmegen, the Netherlands)b is standardised to be 1 cm and ϵ is the molar absorptivity. This value differs for the different materials and even for different AuNP sizes. For 20 nm citrate capped AuNPs an absorption coefficient of $9.51 \times 10^8 \text{ M}^{-1} \text{ cm}^{-1}$ was used at 517 nm.³¹ For 40 nm and 80 nm AuNPs the respective used absorption coefficients were $6.73\text{E}+9$ and $5.54\text{E}+10 \text{ M}^{-1} \text{ cm}^{-1}$.³² Both were taken at 520 nm. With these values the stock concentration C can be calculated. The stock for 40 nm AuNPs, the focus of this thesis, was found to have a concentration of $1,56\text{E}-10 \text{ M}$.*

There are 3 main reasons as to why this test is necessary. First, the measurements will be done in a plate reader. As such, the optical pathlength cannot be assumed to be 1 cm. Second, the plate reader might show different behaviour than the nanodrop system used to find the stock

*This concentration is crucial to multiple experiments, which is why this measurement is covered here instead of the results.

concentration. The third reason is that the AuNPs will be functionalised with multiple molecules such as mPEG, tween20 and DNA, which might alter absorption. As such, this experiment will constitute multiple different conditions that each test absorption under different circumstances.

In order to accurately determine the concentration of AuNPs in the medium, some tests have been carried out. First the 40 nm AuNP concentration in stock has been calculated. Next, a dilution series was made with the AuNPs, diluted in MilliQ water. This series can be seen in table 6 in the appendix.

Two other volumes of stock AuNPs were functionalised. One batch was functionalised with 2 kDa mPEG and one batch with 6 kDa mPEG. This was done by adding 14,1 μ L mPEG was used per 600 μ L AuNPs, creating a solution with 2,35 μ M mPEG, the maximal loading, as determined in chapter 4. 6 μ L tween20 was also added. This was done because both mPEG and tween20 both molecules can influence absorption, as such they can be considered confounding factors. However, the added concentration of tween20 and mPEG does not change across the different experiments. As such, with one measurement their effect can be corrected for.

After incubating, the AuNPs went through 8 washing steps. The same dilution series was kept as for pure AuNPs in MilliQ. However, PBST was used instead of MilliQ. Additionally some volume was added due to functionalisation. The dilution series has been recreated and can be viewed in the appendix (table 7). This induced deviation is also corrected for during analysis of the results.

One problem of this functionalisation is that it might lower the AuNP concentration because of the washing steps. This causes the experiment to lose some reliability. To combat this a calibration curve will also be made using a regular AuNP dilution series. Which dilution series will be used in follow ups is determined by the differences between the curves.

Another problem is DNA loading. This is more complicated than the addition of mPEG and tween20. The conjugation of DNA to the particles slightly influences their absorption. The absorption peak is known to shift laterally up to 2.9 nm based on DNA density, among other factors.³³ This possible lateral shift can be accounted for by taking the absorption at a range of wavelengths, thus creating a spectrum, and then taking the peak absorption. However, there might also be a vertical shift in absorption. Similar experiments utilise normalised absorption to calculate lateral shift. As this is not possible for our experiment DNA binding will be a confounding factor. This will be covered in the results and discussion section, together with the absorption changes because of mPEG and tween20.

Measurements were done by taking the peak absorption for each well. Each measurement was taken in triplicate. Two technical duplicate were also made, resulting in 6 data points per condition. The 3 conditions with the highest AuNP concentration formed an exception. These conditions each had 2 wells and a technical duplicate for 4 data points total. For the highest concentration the entire absorption spectrum was also be measured to find possible peak shift.

5.4 DNA density and mPEG chain length

This experiment utilises the calibration curves created in the previous experiments. The goal is to find the influence of added DNA and mPEG length on the number of DNA strands bound to the AuNPs. To find this, the amount of DNA added is altered to form 4 conditions. Additionally,

each DNA condition will be tested in combination with 2kDa mPEG + tween20 or 6kDa mPEG + tween20. This comes down to a total of 8 conditions.

The first step is a dilution of the AuNPs. The necessary amount of stock is centrifuged at 5000 RCF until the supernatant is clear. $\frac{2}{3}$ of the supernatant is pipetted off. This way the AuNP concentration is increased threefold. Now the AuNP dilution can be divided over eppendorf tubes for each condition. Next, 1% wt tween20 and mPEG is added. since mPEG and tween20 bind to the AuNPs, the concentration of these is increased threefold with respect to the original protocol as well. After incubating for 20 minutes, the desired DNA concentrations can be added (HS-polyA5-GHS35nt-647n, Biolegio, Nijmegen, the Netherlands). The base added concentration is calculated to be 500 strands/AuNP, with additional concentrations of 5, 10 and 20 times the base concentration. Afterwards, NaCl is added and the dilution is incubated in the dark for an hour. All following steps are done in low light conditions, to reduce photobleaching. When the tubes are not actively being pipetted, they are covered to prevent fluorophore degradation.

In contrast to the other added molecules, the added amount of NaCl has not been increased. This is because NaCl is necessary to create a high ionic strength environment. The ions do not bind to the AuNPs, so the concentration does not need to be increased.³⁰ The second reason is more important though. In previous iterations of this experiment (which are covered in more detail in the results). It was found that the citrate capped AuNPs are less stable at higher concentrations. Adding more salt decreases the stability further, making coagulation likely. As such, the choice was made to keep total NaCl concentration low.

After incubating, the volume of each tube is increased by addition of PBST. Next, all excess DNA is washed away. This is done by repeatedly centrifuging for 6 minutes at 5000 RCF, taking 800 μ l supernatant, adding 800 μ l PBST and centrifuging again. After washing 400 μ l supernatant is taken to again increase the AuNP concentration. Next, the actual AuNP concentration is measured by taking 80 μ l aliquots out of each tube and measuring absorption in the plate reader. The concentration can be calculated using the calibration curves, found in a previous experiment.

After taking 80 μ l for the absorption measurement, MCE is added to each tube. After this step the AuNPs are incubated overnight in a dark place. The next morning fluorescence can be measured in triplicate. The fluorescence can be related to concentration by a calibration curve found in a previous experiment. Lastly the entire experiment is repeated to create a technical duplicate.

5.5 ssDNA binding to HS-DNA on AuNPs

This experiment is based on previous experiments. As such, the protocol is very similar to the previous experiments. The protocol for experiment 4 (section 5.4) is repeated up to the washing steps. There is one difference. Instead of fluorescent labelled HS-DNA, regular HS-DNA is used. (HS-polyA5-GHSR35m, Eurofin genomics, Leiden, the Netherlands) After washing the particles are functionalised and stable. In contrast to the previous experiment, there is no additional centrifuge step, and the total volume is kept at 1000 μ l. No aliquots are taken for the absorption measurement.

Instead, the following steps are done: First, fluorescent target DNA is added. (targetshortGHSR35nt-647n, Eurofin genomics, Leiden, the Netherlands) To avoid making another calibration curve the same fluorescent label should be used as in earlier experiments. Second, the chosen target DNA should be specific and complementary to the HS-DNA added in the previous step. This experiment

simulates the ssDNA detection method as described in chapter 4, although ssDNA is added in a known quantity. target DNA is added in a 100-fold excess in relation to the measured number of HS-DNA strands in experiment 4. After adding target DNA washing steps are conducted. As in previous experiments, these washing steps should be done in low light conditions to avoid photo-bleaching. The eppendorf tubes are washed a total of 7 times.

After washing, the experiment proceeds the same way as experiment 4. The tubes are centrifuged an additional time and 600 μ l supernatant is taken. After shaking, 80 μ l aliquots are taken and absorption is measured. Next, 1,56 μ l MCE is added and the tubes are set to incubate overnight at room temperature. The next morning 100 μ l is taken three times and fluorescence is measured thrice for each condition. Additionally, a blanco measurement is done. This is done by following the same experiment except no HS-DNA is added. After measurements are taken, the results can be calculated using the previous calibration curves.

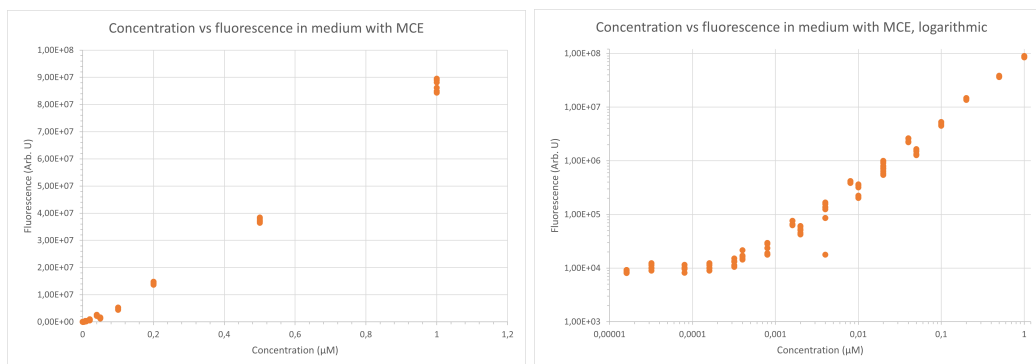
6 RESULTS AND DISCUSSION

In this section the results of the experiments are covered. The calibration curve for A647n is discussed first. Next the gold nanoparticle calibration curve and the related gold nanoparticle stability are illustrated. Using these results the last two experiments were done. These are related to HS-DNA and target DNA conjugation. The created calibration curves are used to analyse the results of these experiments. Each experiment is analysed and discussed in its own subsection. Each section will end with some concluding remarks.

6.1 Fluorescence calibration

Fluorescence was measured in two conditions; in pure PBS and in PBST with added MCE. As the curve made in the solution with PBST and MCE is more accurate with respect to the conditions in the wells after the protocol, this curve will be discussed in depth.

For fluorescence in MCE a dilution series was made. This series was not only used to find the calibration curve but also to find the limit of detection (L.O.D) and the limit of quantification (L.O.Q.). This was done by diluting to concentrations well below the expected L.O.D. Fig 4 shows the dilution series using a logarithmic scale. As can be seen, there is a clear linear correlation between fluorescence intensity and DNA concentration down to a certain level. After that the measured intensity stays the same, unrelated to the DNA concentration.



(a) A linear plot relating a647n concentration and fluorescence. Each dot represents a data-point
 (b) A logarithmic plot that relates a647n concentration and fluorescence. The lower concentrations are more visual than in a linear plot. Note the LOD is clearly visible

Figure 4: Fluorescence of a647n in medium with mercaptoethanol

The border at which measured fluorescence is still correlated to the fluorophore concentration is the L.O.D. The L.O.D. was detected in two ways. Visually, the L.O.D. is found to lie between 0,3 and 0,6 nM. The L.O.D. is determined to be 5,25 nM at 95% confidence, using the linear regression method. Chapter 10.3 shows the calculations done to find the L.O.D.

The limit of quantification (L.O.Q.) is related to the L.O.D. However, it measures at which concentration the correlation between fluorescence and DNA is linear. In other words: the point at which a linear fit is accurate, and quantitative statements can be made about the concentration. The L.O.Q. is found to be 15,90 nM.(see chapter 10.3)

The calibration curves as seen in figure 5 show that for the experiment with MCE fluorescence was higher than in pure PBS. This is unexpected, as MCE is known to be either unreactive, or to have quenching effect on specific fluorophores.³⁴

Although the higher fluorescence was unexpected, it was the most accurate curve since MCE will be present following AuNP functionalisation. The difference in temperature across the measurements could be a reason for the altered fluorescence in MCE treated a647n as opposed to untreated fluorophore. For MCE, the temperature was 23 and 25.5 ± 0.5 °C. For the measurement in PBS the temperature was 20.5 °C.

Based on figures 4 and 5 and an equation has been made using the linear part of the dilution series to approximate the linear relationship between fluorescence and concentration. The equation is:

$$C = F * 1.17 * 10^{-8} + 0.01132659959 \quad (5)$$

In which C is the concentration in micromole per liter and F is the fluorescence (Arbitrary units). This equation will be used in follow-up experiments to determine Fluorescent DNA concentrations based on the intensity.

concluding remarks on fluorescence

based on the dilution series, a calibration curve has been set up for fluorescence in PBST and MCE. The L.O.Q. was found to be 15,90 nM, while the L.O.D. was determined to be 5,25 nM. Using the calculated L.O.D. and the L.O.D. found optically, it was deemed safer to alter the original protocol by adding one extra washing step for max added DNA. That way the DNA concentration in the wells is well below the detectable amount.

6.2 AuNP stability when coated with mPEG and tween20

In order to verify AuNP stability, two experiments have been carried out. For the first experiment the particles were coated with different mPEG concentrations, after which NaCl was added. For the second experiment tween20 was also added. The experiments were done for both 2kDa and 6kDa mPEG. Figure 7 shows stability for different mPEG concentrations in high ionic strength ($>1M$ NaCl) solution, while figure 6 shows a reference picture for stable AuNPs.

After incubating figure 7 was made to show stability. As can be seen, AuNPs with 2kDa mPEG coagulate no matter the concentration. This is lower than the theory, which states mPEG

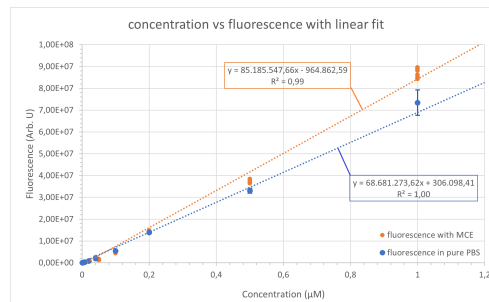


Figure 5: The linear part of the calibration curve for fluorescence with MCE. The curve in PBS has also been included for comparison

concentrations of 0,05 μM and higher should result in brush conformation and stabilise the AuNPs. A possible cause is very low binding efficiency for the molecules, making the AuNPs more sparsely covered than expected. It is also possible the 2kDa chains are not long enough to keep the AuNPs from coagulating, no matter their conformation.



Figure 6: Untreated AuNPs, as a reference for the colour all samples had before adding NaCl and incubating.

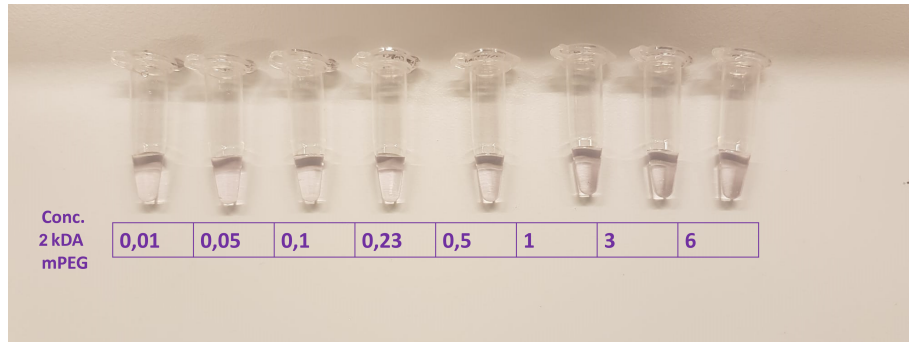
The particles are stable when 6kDa mPEG is conjugated. This is as expected. Since each molecule is longer, the same added concentration results in more steric effect. To find when mPEG chains do fail in keeping the AuNPs from coagulating more salt was added. Adding salt increased the concentration from 1,16 M to 1,47 M. After adding extra salt, the AuNPs loaded with up to 0.1 μM mPEG showed coagulation. The other tubes show some discolouration but this is likely an effect of the added volume.

Another possible surface molecule is tween20. In a follow-up on the previous experiment, the same conditions were followed. However, tween20 was also added to find how the particles behave when coated with both molecules. It was hypothesised tween20 has an additional stabilising function.¹⁹ After following the protocol and incubating, pictures were taken. These can be seen in figure 8, again 6kDa mPEG is stable at all concentrations added. This is as expected since they were already stable without added tween20.

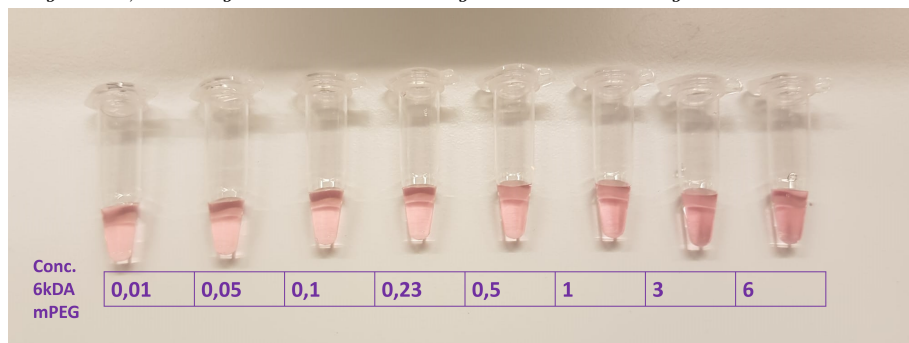
As can be seen in figure 8a, the particles are more stable at mPEG concentrations of 0,1 μM and higher for 2kDa mPEG. This is a high contrast to not being stable at any concentration without added tween20. For 6kDa, the tubes' colour shows AuNPs are stable at all mPEG concentrations, as is expected. Without tween20, 6kDa already showed this stability; adding tween20 does not degrade the functionality of the mPEG chains.

Conclusion for needed mPEG & tween20 concentration The experiments have shown that the combination of tween20 and mPEG can ensure nanoparticle stability when used in conjunction with either chain length, as long as the added mPEG concentration is higher than 0,1 μM for 2kDa mPEG. For 6kDa mPEG, all concentrations are stable. Now, a fitting concentration to be used in follow-up experiments can be chosen.

The ideal concentration for follow-ups needs to be well above the minimal needed concentration found in this experiment. It also needs to be below the theoretical maximal loading for 6kDa as found in chapter 4.4. This will ensure loading is equal among all AuNP types and conditions. Based on these factors an added mPEG concentration of 2,35 μM has been chosen for 40 nm AuNPs. This concentration corresponds to a density of 3 strands/ nm^2 .



(a) Tubes filled with gold colloid, coated with 2kDa mPEG chains. The concentration is in μM . As can be seen, all are light blue, meaning the AuNPs have coagulated under the high salt concentration.

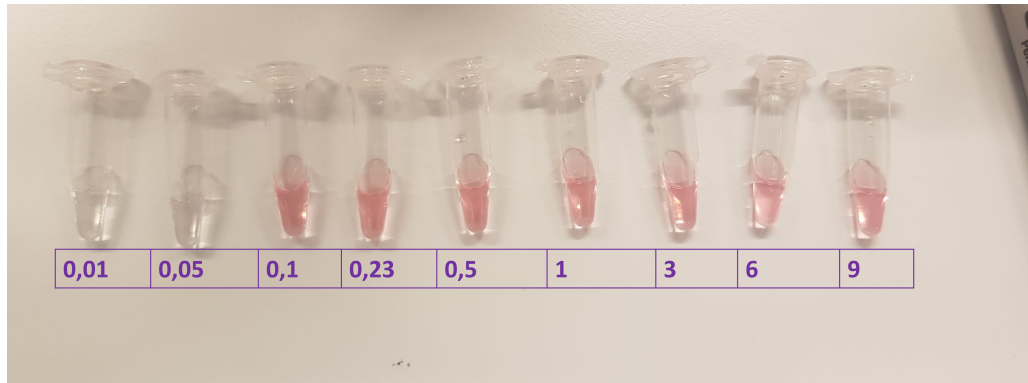


(b) Tubes filled with gold colloid, coated with 2kDa mPEG chains. The concentration is in μM . As can be seen, the colloid remains stable at these salt concentrations

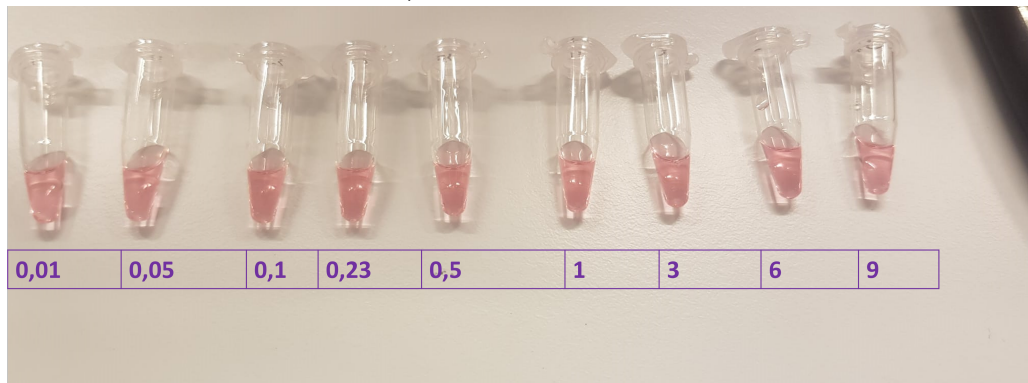


(c) The salt concentration for 6kDa mPEG was increased with as a result that with low mPEG concentrations the AuNPs dit start to coagulate.

Figure 7: Different mPEG lengths and salt concentrations. Red indicates a stable colloid while clear indicates that particles have coagulated.



(a) AuNPs coated with 2kDa mPEG and tween20. The concentrations, in μM , are denoted below the tubes. notice the stability is reached within a $0.1 \mu\text{M}$ mPEG concentration.



(b) AuNPs coated with 6kDa mPEG and tween20. All tubes are red, indicating the AuNPs are all stable.

Figure 8: AuNPs at a $>1\text{M}$ NaCl concentration. The AuNPs were coated with two different mPEG chain lengths and tween20.

6.3 Gold nanoparticle calibration curve

Multiple experiments were done to find the relation between AuNP concentration and absorbance. First, the stock concentration for the gold nanoparticles needed to be determined. This was done by measuring absorbance in a cuvette. The stock concentration was found to be $1,5617\text{E}-10$ M.

Based on this value a calibration curve was made for pure AuNPs. However, as explained in chapter 5.3, the addition of tween20 and mPEG might alter absorption. New calibration curves were made using known AuNP concentrations for coated AuNPs. Using measured absorption both possible lateral and possible vertical peak shifts can be found.

There is a significant lateral peak shift for coated particles with respect to pure AuNPs. When measured with steps of 5nm, the pure AuNPs exhibit a (local) maximum consistently at around

525 nm, while for both coated AuNPs the absorption peak lies around 530 nm. As a follow-up the absorption peaks for coated AuNPs were determined at 1 nm resolution. The peak for the particles coated with tween20 and 2kDa mPEG was found to be 529 nm, while the absorption peak was located at 530 to 532 nm for particles coated with tween20 and 6kDa mPEG.[†]

The absorption peak is not always located at 530 nm. At or below concentrations of $9,43\text{E-}12$ M, peak absorption is sometimes measured at 400 nm. In these cases there is a local high point at 530 nm. The intensity of this peak decreases based on concentration. As such, the high point at 400 nm is likely not due to the AuNPs but due to something unrelated like the solution.

Based on the data delivered by the absorption peaks the dilution series was created at 530 nm. The data points plotted in figure 9. The lowest concentration are shown to be, on average, lower than the blanco measurements. This indicates these concentrations cannot be detected. As such, all data points below $2,36\text{E-}12$ M have been left out when creating the linear fits.

figure 10 shows the absorption for all three conditions. There is a small decrease in absorption for mPEGylated AuNPs. This is slightly more so for those activated with longer mPEG chains. Do note that while these measurements more accurately represent the actual measuring conditions in following experiments, they are also less precise due to the additional steps in the protocol and a lower number of measurements (4 to 6 as opposed to 9 for pure AuNPs). A Two-sample T-test done on at the maximal concentration showed there was no significance between the two mPEGylated AuNP types.

The linear fits can be rewritten to give concentration, based on absorption at 530 nm. As long as the same conditions are being used. This formula for 2kDa coated AuNPs goes:

$$C_{\text{AuNP},2\text{kDa}} = A * 7.72 * 10^{-10} - 3.09 * 10^{-11} \quad (6)$$

For AuNPs coated with 6kDa mPEG, the process is much the same, with the following formula as end result:

$$C_{\text{AuNP},6\text{kDa}} = A * 7.99 * 10^{-10} - 3.19 * 10^{-11} \quad (7)$$

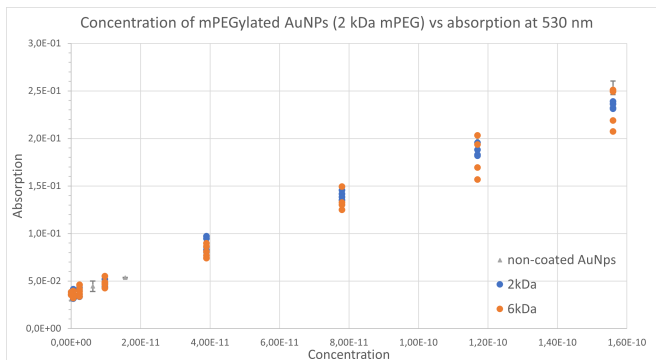


Figure 9: The data points for the dilution series

[†]For those interested, the maximum absorption for each condition is covered more extensively in the appendix.

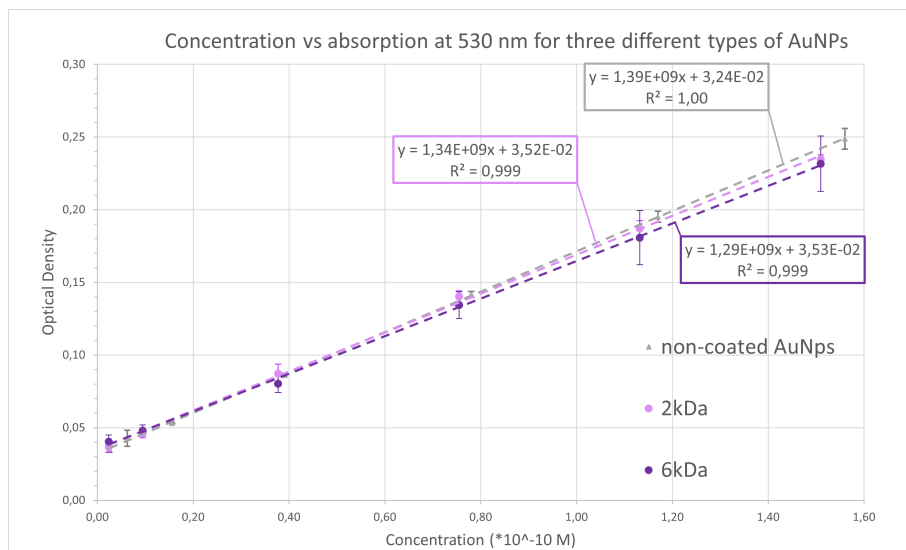


Figure 10: The linear fits for the absorption with the two mPEG lengths. The formulas and R^2 values are also shown.

concluding remarks on AuNP absorption

In short: there is a clear lateral peak shift for mPEG functionalised AuNPs. It is shown that the absorption peak for 40 nm AuNPs shifts from 525 to 530 nm. There is no significant vertical peak shift. While following experiments use the calibration curves for each condition, any future protocols can use the absorption for pure AuNPs to create a calibration curve. This is possible as this thesis has proven that there is no significant difference in absorption at 530 nm.



Figure 11: The tubes after overnight incubation. this picture is representative for all conditions

6.4 Optimal HS-DNA loading on AuNPs

In this section, the optimal HS-DNA loading on AuNPs will be covered. To find optimal HS-DNA binding both the amount of added DNA and two different mPEG lengths were tested, as described in chapter 5.4.

For the protocol, the AuNP concentration was increased threefold with respect to previous experiments, as was the concentration for surface molecules and HS-DNA. This was done to increase the amount of HS-DNA per well for the same number of strands per AuNP. The effect of this change is that the plate reader can detect more fluorescence, and thus detect a lower number of strands/AuNP. This increase was necessary as in previous experiments no strands were detected.

The problem with increasing AuNP concentration is that stability is decreased, as found during the gold nanoparticle stability experiment (see section 6.2). Consequently, the salt concentration could not be increased without increasing risk of coagulation. Even with the addition of mPEG and tween20, there is a high likelihood the AuNPs will coagulate overnight. This was experimentally found to be one of the main problems in the follow-up experiment.

After measuring absorption of functionalised AuNPs MCE was added. MCE removes all surface molecules, as was necessary in order to measure fluorescence. Removing surface molecules decreased AuNP stability. This affected stability as all tubes showed coagulation after overnight incubation. This can also be seen in figure 11. This is no problem, since all DNA is free floating.

Based on the absorption measurements, the fluorescence measurements and the calibration curves, figures 12 and 13 were made. These figures show the number of HS-DNA strands per AuNP for different conditions and mPEG chain lengths. For higher clarity, this is also shown in table 14. The figures also show the limit of quantification (upper black bar) and the limit of detection (lower black bar). These cutoff values are dependent on a set fluorescence value, however they still appear at a different number of strands/AuNP, because the gold nanoparticle concentration differs across measurements. This is an effect of small losses during the washing steps and unfortunately unavoidable.

For 2kDa, there is a small increase in loading at higher added DNA concentrations. However, the number of DNA strands per AuNP was below the limit quantification for each condition. As such the actual value can be only with certainty determined to be between the LOD and LOQ for each condition.

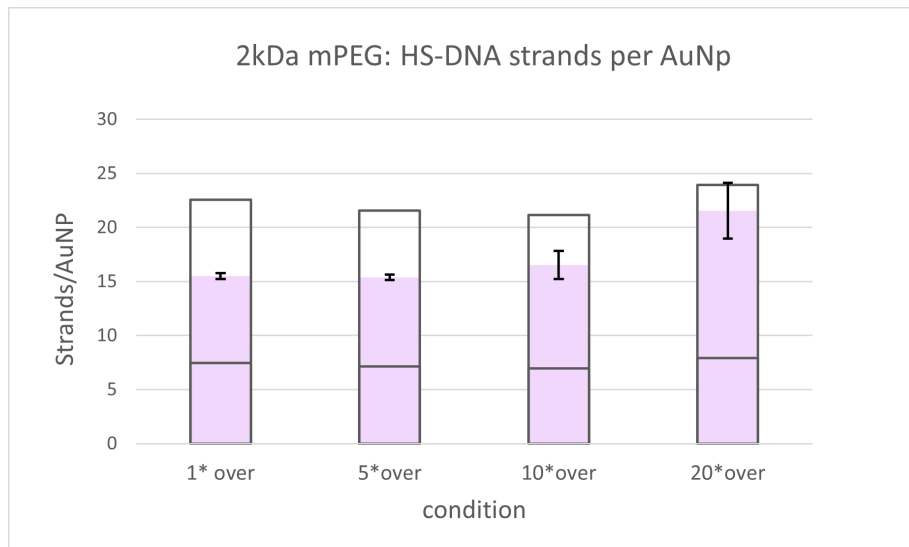


Figure 12: A bar graph showing DNA loading on AuNPs coated with 2kDa mPEG. For 2kDa the values all fall below the limit of quantification. The number of strands/AuNP detectable at the LOD is shown with a black outline.

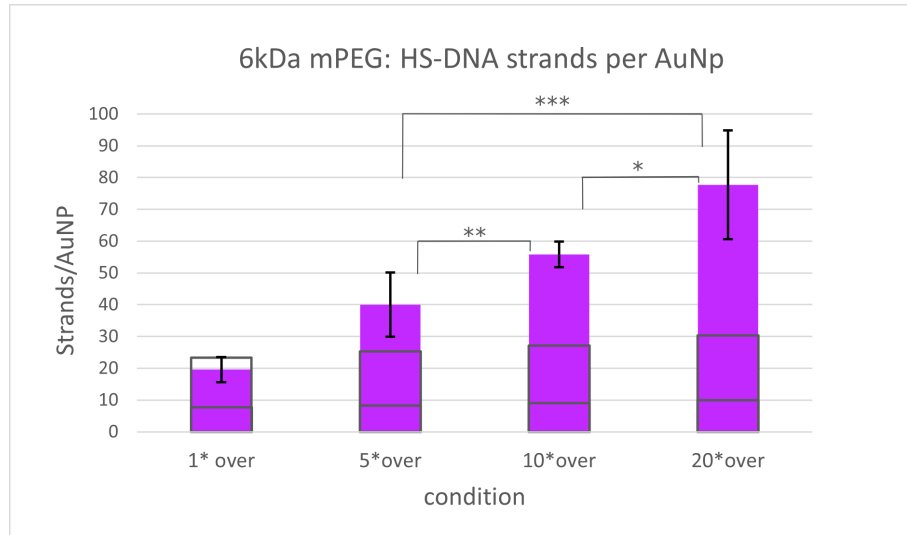


Figure 13: A bar graph showing DNA loading on AuNPs coated with 6kDa mPEG. Note asterisks show significance. One to four asterisks show 95%,97.5%,99% and 99.9% confidence respectively. Significance is not calculated for values below the L.O.Q (as calculated using the linear regression). For these values, the L.O.D is shown to denote the minimal number of strands/AuNP that can be measured

mPEG	2kDa	2kDa	2kDa	2kDa	6kDa	6kDa	6kDa	6kDa
Added DNA (500 strands/np)	1*	5*	10*	20*	1*	5*	10*	20*
Detected DNA conc.	1,09E-08	1,14E-08	1,24E-08	1,43E-08	1,54E-08	2,50E-08	3,25E-08	4,00E-08
Average detected strands/np	15,5	15,4	16,5	21,5	19,6	40,1	55,8	77,8
Standard deviation	0,267	0,239	1,304	2,580	3,939	10,143	4,025	17,105

Figure 14: The average number of strands per AuNP with different length mPEG surface molecules and various DNA concentrations added. The error bars show one standard deviation.

For 6kDa, the 1* over condition also has DNA detection below the limit of quantification. The three higher conditions for 6kDa are well above detection limits, as can be seen in figure 13. As such the loading for these conditions can be determined accurately. It is expected loading increases up to a certain point after which DNA loading experiences a platform. This happens because max loading is reached. The results for 6kDa functionalised AuNPs indeed showed a significant increase in DNA loading with each condition, however the platform has not been found. The maximal loading (at 20* max DNA added) showed up to 78 strands/AuNP. This is still below the theorised max loading of 500 strands/AuNP.

absorption increase

With the standard protocol and the original amount of salt, the functionalised AuNPs were mostly stable. Absorption was measured immediately after functionalisation and after one night of incubation. The absorption after overnight incubation was significantly higher, across all measured conditions. We have chosen to use the data after one night of incubation. Increasing absorption suggest coagulation took place. However in contrast to these results, there were no indicators of coagulation. The wells appeared optically identical. Changes as seen in figure 8a were not recorded. More research is needed to find what caused the increase in absorption.

concluding remarks

Overall, this experiment shows 2kDa mPEG is a poor surface molecule for direct DNA conjugation. For 6kDa DNA loading was significantly higher at all concentrations, except 1* over. Thus far, 6kDa and 20* over show the highest DNA loading. A maximum has not yet been found. More research is needed to find this maximum and to find what causes the absorption increase after incubating.

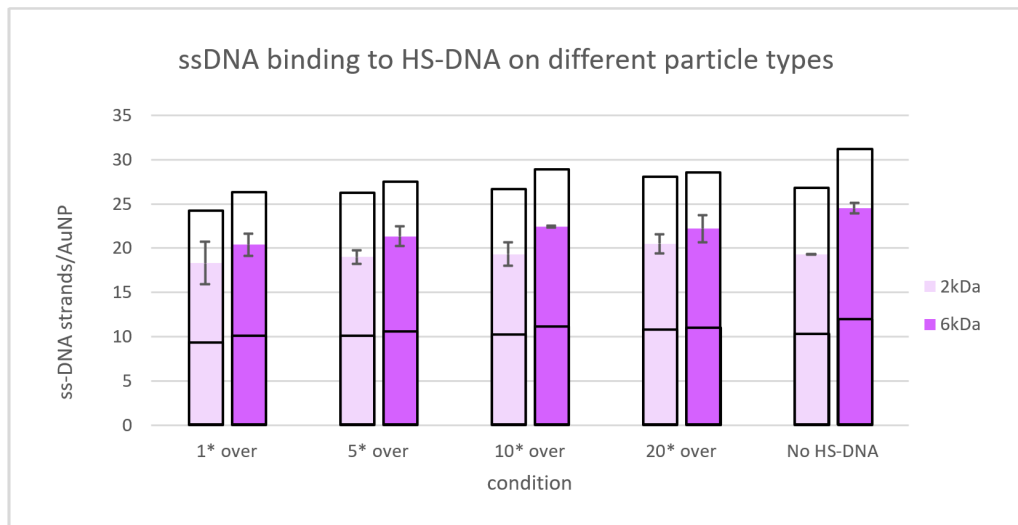
6.5 Optimal target DNA loading

In the last experiment the number of HS-DNA strands per AuNP for different conditions was derived. The end goal, however, is to find the number of target DNA strands that can bind to the AuNPs. To determine this a last experiment was set up. The same conditions as in the previous experiments are used to conjugate HS-DNA. Only in this experiment, the HS-DNA is not fluorescent but it is complementary to a fluorescent target DNA strand. For target DNA addition, a hundredfold excess was chosen in relation to the highest number of HS-DNA strands per AuNP found in the previous experiment.

After incubating and washing, fluorescence was measured. Expectations were that the amount of target DNA would increase with increasing HS-DNA concentration, up to a certain optimum. After that, steric effects due to the sheer number of HS-DNA strands takes over and hinders target DNA binding. As can be seen in figure 15a, the results were not as expected. There was no increase in fluorescence measured across conditions. Table 15b shows the detected fluorescence is indeed well below the determined L.O.Q but above the L.O.D found using linear regression. For additional certainty, the conditions are compared to blanco measurements. These blancos were made using just BPS and MCE, without any AuNPs or fluorescent molecules. This can be seen in the appendix, chapter 10.7.2.

The measured fluorescence, the L.O.D. and the L.O.Q. are in agreement. In all likelihood, there is indeed fluorescence being detected, However, measured fluorescence is very similar across

conditions. Additionally, there is fluorescence being detected in wells containing no HS-DNA. In these wells target DNA is not able to bind. As such, we can assume any detected fluorescence is not due to target DNA that was bound to the HS DNA.[‡]



(a) A bar chart showing the number of target DNA strands per AuNP for different added HS-DNA concentrations. Target DNA is added in excess with respect to the highest number of HS-DNA strands per AuNP found. Note there is no significant difference in strands/NP across conditions.

mPEG	2kDa	2kDa	2kDa	2kDa	2kDa blanco	6kDa	6kDa	6kDa	6kDa	6kDa blanco
Detecte d DNA conc.	1,15E-08	1,15E-08	1,15E-08	1,16E-08	1,15E-08	1,23E-08	1,23E-08	1,24E-08	1,25E-08	1,25E-08
strands /np	18,31	18,98	19,33	20,48	19,33	20,39	21,34	22,43	22,19	24,50
St. dev	2,410	0,738	1,330	1,098	0,037	1,271	1,124	0,123	1,541	0,586

(b) The measured fluorescence, standard deviation and number of strands per particle

If there is no fluorescence detected, something else must cause the fluorescent results. There is one type of fluorescent molecule in the wells, namely the A647n labeled target DNA. With this in mind the results suggest there is free floating DNA in the wells. However, checking the protocol showed the washing steps suggest a fluorophore concentration of roughly two orders of magnitude

[‡]otherwise the measurements without HS-DNA added would be lower than the other conditions

below the L.O.D. found using linear regression. Therefore, this cannot be the cause for fluorescence. The calculations have been included in the appendix; chapter 10.7.2.

A possible cause for these results is aspecific binding of the target DNA to the AuNPs. this explains why DNA is bound regardless of HS-DNA addition. Of course, there are other possibilities that might cause these results. Another molecule in the tubes could be fluorescent for example. However, this is very unlikely as the wells do not contain any molecules known to be fluorescent.

concluding remarks

In short, the amount of target DNA bound to the AuNPs in this experiment is lower than the LOD. Few can be said about a possible optimum. Only that the binding is not 100 % efficient. Otherwise the results would be very similar to the results found in the previous experiment.

7 CONCLUSION

The goal of this thesis was to optimise target DNA loading on gold nanoparticles. First, absorption for the different AUNP types was measured. There is a significant peak shift, based on AuNP loading. absorption intensity changes little. measuring pure AuNPs at the peak wavelength for coated AuNPs is a valid strategy. A further experiment was done regarding stability. It was shown AuNPs coated with mPEG and tween20 are stable in high ionic strength solutions, if the added mPEG concentration is above 0,1 μM . However, at high AuNP concentrations the results indicate stability is lowered. AuNPs were coated with two mPEG lengths. Different HS-DNA concentrations were added to find differences in HS-DNA conjugation. The results showed 6kDa mPEG has a significant increase in DNA loading at higher added HS-DNA concentrations. Lastly, target DNA loading was measured. The results did not show differences between the different conditions and the blanks. More research is needed to find the optimal surface molecules and HS-DNA concentration for binding target DNA.

8 OUTLOOK

8.1 Future research

6kDa AuNPs show an increase in loading with increasing HS-DNA concentrations but a maximum or steady state has not yet been found. For 2kDa, there is no clear increase in loading at the HS-DNA concentrations added. As such, a possible follow up can possibly test HS-DNA binding on different AuNPs, but with higher added concentrations. This way maximal HS-DNA conjugation to AuNPs can be found for different AuNP types.

Following up on increased HS-DNA concentrations; much the same is true for target DNA binding. Thus far, any target DNA binding could not be determined. A possible, if not necessary, experiment can be set up using higher target DNA concentrations. Additional precautions can be taken to ensure detectable fluorophore levels, such as: changing to a brighter fluorophore and/or increasing AuNP concentration again. However, increasing AuNP concentration will deliver diminishing results without an altered protocol. Keep in mind the maximum absorption that can be detected by the plate reader (up to an O.D. of 3 for the spectramax ID5³⁵). More importantly, this research found AuNP stability decreases when concentration increases. In order to increase concentration further, another method needs to be found that stabilizes the AuNPs and does not interfere with the measurements.

The last important change is a follow up experiment that measures absorption over time for different AuNP types. Experiments in this thesis found AuNP absorption increases after overnight incubation for functionalised AuNPs.

Additional experiments can be done by changing surface molecules. As of yet tween20, 2kDa and 6kDa mPEG are used. An experiment with 0.8 kDa mPEG was set up, but this was not possible due to delivery constraints. As such the protocol is set up with 0.8 kDa in mind.

Lastly, after the protocol is optimised using fluorescent labelled DNA, it still needs to prove effective in more realistic conditions. In other words, in an experiment that uses two types of AuNPs and notes different efficiencies for target DNA to bind them together.

8.2 implications

Although more research is needed to find optimal target DNA binding, there are findings that can be used in future research.

First, this thesis has shown that while there are differences, creating a calibration curve using pure AuNPs is a valid alternative to creating calibration curves with AuNPs coated with surface molecules. This is true as long as the lateral peak shift is taken into account. Furthermore, this research has shown the L.O.D. for A647n fluorescence in the spectramax ID3 plate reader. In accordance with this finding, it has been shown an additional washing step was needed at the highest added HS-DNA concentration in the original protocol. Lastly, this thesis covered AuNP stability in high ionic strength solutions. This research has shown AuNPs are stable in >1 M NaCl solutions when 0,1 μ M 2kDa mPEG and tween20 is added. It has also shown the same level of stability can be reached at lower mPEG concentrations, as long as the molecular weight of mPEG is increased.

9 ACKNOWLEDGEMENTS

Figures 1 and 3 are made using biorender. The original protocol, as seen in section 16. Is an adapted version of the protocol in Li et al. (2014)¹, edited by Dr. Ir. J.E. van Dongen.

I gratefully acknowledge Dr. Ir. J.E. van Dongen (BIOS, Lab-on-a-chip-group, University of Twente) for her daily supervision, insight and endless patience. I would like to thank Prof. Dr. Ir. L.I. Segerink (BIOS, Lab-on-a-chip-group, University of Twente) for her enthusiasm and flexibility, and Prof. Dr. A. Kocer (BioEE, University of Twente) for her enthusiasm, flexibility and steady stream of questions, forcing me to consider all possibilities!

Bibliography

- [1] Li J, Zhu B, Yao X, Zhang Y, Zhu Z, Tu S, et al. Synergetic Approach for Simple and Rapid Conjugation of Gold Nanoparticles with Oligonucleotides. *ACS Appl Mater Interfaces*. 2014 Oct;6(19):16800-7.
- [2] Sung H, Ferlay J, Siegel RL, Laversanne M, Soerjomataram I, Jemal A, et al. Global Cancer Statistics 2020: GLOBOCAN Estimates of Incidence and Mortality Worldwide for 36 Cancers in 185 Countries. *CA Cancer J Clin*. 2021 May;71(3):209-49.
- [3] Pulumati A, Pulumati A, Dwarakanath BS, Verma A, Papineni RVL. Technological advancements in cancer diagnostics: Improvements and limitations. *Cancer Reports*. 2023 Feb;6(2).
- [4] Sarhadi VK, Armengol G. Molecular Biomarkers in Cancer. *Biomolecules*. 2022 Aug;12(8).
- [5] Li Y, Mansour H, Wang T, Poojari S, Li F. Naked-Eye Detection of Grapevine Red-Blotch Viral Infection Using a Plasmonic CRISPR Cas12a Assay. *Anal Chem*. 2019 Sep;91(18):11510-3.
- [6] Verdoold R, Gill R, Ungureanu F, Molenaar R, Kooyman RPH. Femtomolar DNA detection by parallel colorimetric darkfield microscopy of functionalized gold nanoparticles. *Biosens Bioelectron*. 2011 Sep;27(1):77-81.
- [7] López-Valls M, Escalona-Noguero C, Rodríguez-Díaz C, Pardo D, Castellanos M, Milán-Rois P, et al. CASCADE: Naked eye-detection of SARS-CoV-2 using Cas13a and gold nanoparticles. *Anal Chim Acta*. 2022 May;1205:339749.
- [8] Kelly KL, Coronado E, Zhao LL, Schatz* GC. The Optical Properties of Metal Nanoparticles: The Influence of Size, Shape, and Dielectric Environment. *ACS Publications*. 2002 Dec.
- [9] Yoon JH, Selbach F, Schumacher L, Jose J, Schlücker S. Surface Plasmon Coupling in Dimers of Gold Nanoparticles: Experiment and Theory for Ideal (Spherical) and Nonideal (Faceted) Building Blocks. *ACS Photonics*. 2019 Feb.
- [10] Liu B, Liu J. Methods for preparing DNA-functionalized gold nanoparticles, a key reagent of bioanalytical chemistry. *Anal Methods*. 2017 May;9(18):2633-43.
- [11] Bedford EE, Spadavecchia J, Pradier CM, Gu FX. Surface Plasmon Resonance Biosensors Incorporating Gold Nanoparticles. *Macromol Biosci*. 2012 Jun;12(6):724-39.

- [12] Ma X, Li X, Luo G, Jiao J. DNA-functionalized gold nanoparticles: Modification, characterization, and biomedical applications. *Front Chem.* 2022 Dec;10:1095488.
- [13] van Dongen JE. Novel Biosensors for early Cancer Detection: Development of Gold Nanoparticle and Crispr/Cas Assays for the Optical Detection of Cancer Biomarkers in Urine [dissertation]; 2022.
- [14] Mayer KM, Hafner JH. Localized Surface Plasmon Resonance Sensors. *Chem Rev.* 2011 Jun;111(6):3828-57.
- [15] Kelly KL, Coronado E, Zhao LL, Schatz GC. The Optical Properties of Metal Nanoparticles: The Influence of Size, Shape, and Dielectric Environment. *J Phys Chem B.* 2003 Jan;107(3):668-77.
- [16] Muri HI, Hjelme DR. LSPR Coupling and Distribution of Interparticle Distances between Nanoparticles in Hydrogel on Optical Fiber End Face. *Sensors (Basel, Switzerland).* 2017 Dec;17(12).
- [17] Kasputis T, Hilaire SS, Xia K, Chen J. Colorimetric Detection of Antimicrobial Resistance from Food Processing Facilities Using a CRISPR System. *ACS Food Sci Technol.* 2023 Jan;3(1):17-22.
- [18] CARLROTH. Tween® 20, 250 g, CAS No. 9005-64-5 | Buffer salts for molecular biology | Molecular biological buffers | Reagents for Molecular Biology | Molecular Biology | Life Science | Carl Roth - International; 2023. [Online; accessed 26. May 2023]. Available from: <https://www.carlroth.com/en/buffer-salts-for-molecular-biology/tween-20/p/9127.1>.
- [19] Basso CR, Crulhas BP, Castro GR, Pedrosa VA. A Study of the Effects of pH and Surfactant Addition on Gold Nanoparticle Aggregation. *J Nanosci Nanotechnol.* 2020 Sep;20(9):5458-68.
- [20] Borzenkov M, Chirico G, D'Alfonso L, Sironi L, Collini M, Cabrini E, et al. Thermal and Chemical Stability of Thiol Bonding on Gold Nanostars. *Langmuir.* 2015 Jul;31(29):8081-91.
- [21] solutions B. Gold Colloid: 40nm -500ml - BBI Solutions | Lateral Flow, Reagents and POCT; 2023. [Online; accessed 14. May 2023]. Available from: <https://www.bbisolutions.com/en/product/gold-colloid-40nm-500ml1>.
- [22] Liu H, Doane TL, Cheng Y, Lu F, Srinivasan S, Zhu JJ, et al. Control of Surface Ligand Density on PEGylated Gold Nanoparticles for Optimized Cancer Cell Uptake. *Part Part Syst Char.* 2015 Feb;32(2):197-204.
- [23] Rahme K, Chen L, Hobbs RG, Morris MA, O'Driscoll C, Holmes JD. PEGylated gold nanoparticles: polymer quantification as a function of PEG lengths and nanoparticle dimensions. *RSC Adv.* 2013 Apr;3(17):6085-94.
- [24] Rahme K, Chen L, Hobbs RG, Morris MA, O'Driscoll C, Holmes JD. Correction: PEGylated gold nanoparticles: polymer quantification as a function of PEG lengths and nanoparticle dimensions. *RSC Adv.* 2017;7(15):8798-9.
- [25] Damodaran VB, Fee CJ, Ruckh T, Popat KC. Conformational Studies of Covalently Grafted Poly(ethylene glycol) on Modified Solid Matrices Using X-ray Photoelectron Spectroscopy. *Langmuir.* 2010 May;26(10):7299-306.
- [26] Cruje C, Chithrani D. Polyethylene Glycol Density and Length Affects Nanoparticle Uptake by Cancer Cells. *Journal of nanomedicine research.* 2014 Oct;1(1). [Online; accessed 13. Sep. 2023].

- [27] Hill HD, Millstone JE, Banholzer MJ, Mirkin CA. The Role Radius of Curvature Plays in Thiolated Oligonucleotide Loading on Gold Nanoparticles. *ACS Nano*. 2009 Feb;3(2):418-24.
- [28] Hwu S, Garzuel M, Forró C, Ihle SJ, Reichmuth AM, Kurdzesau F, et al. An analytical method to control the surface density and stability of DNA-gold nanoparticles for an optimized biosensor. *Colloids Surf, B*. 2020 Mar;187:110650.
- [29] Hurst SJ, Lytton-Jean AKR, Mirkin CA. Maximizing DNA Loading on a Range of Gold Nanoparticle Sizes. *Anal Chem*. 2006 Dec;78(24):8313-8.
- [30] Mirkin CA, Letsinger RL, Mucic RC, Storhoff JJ. A DNA-based method for rationally assembling nanoparticles into macroscopic materials. *Nature*. 1996 Aug;382(6592):607-9.
- [31] Dolinnyi AI. Extinction coefficients of gold nanoparticles and their dimers. Dependence of optical factor on particle size. *Colloid J*. 2017 Sep;79(5):611-20.
- [32] Kim DK, Hwang YJ, Yoon C, Yoon HO, Chang KS, Lee G, et al. Experimental approach to the fundamental limit of the extinction coefficients of ultra-smooth and highly spherical gold nanoparticles. *Phys Chem Chem Phys*. 2015;17(32):20786-94.
- [33] Lee J, Lee S. Non-Invasive, Reliable, and Fast Quantification of DNA Loading on Gold Nanoparticles by a One-Step Optical Measurement. *Anal Chem*. 2023 Jan.
- [34] Cloin BMC, De Zitter E, Salas D, Gielen V, Folkers GE, Mikhaylova M, et al. Efficient switching of mCherry fluorescence using chemical caging. *Proc Natl Acad Sci USA*. 2017 Jul;114(27):7013.
- [35] LLC MD. SpectraMax iD3 and iD5 Multi-Mode Microplate Readers; 2023. [Online; accessed 24. Oct. 2023]. Available from: <https://www.moleculardevices.com/products/microplate-readers/multi-mode-readers/spectramax-id3-id5-readers#specifications-options>.

10 APPENDIX

10.1 Original protocol

Version: January 28th, 2021
Nienke van Dongen, BIOS lab on a chip group

Protocol for conjugation of Gold Nanoparticles (AuNPs) with ssDNA

1 day synthesis (end overnight incubation for quantification purposes)

Timeline:

Day 1 – Prepare AuNPs

1. Prepare mPEG solution and pre-coat AuNPs (30 minutes including 20 minutes waiting)
2. add the HS-DNA and NaCl (70 minutes, including 60 minutes waiting step)
3. Wash the AuNPs (~60 minutes, depending on the number of samples you are preparing simultaneously.)

Day 2 – (Optional) Quantify DNAs on AuNPs

Needed:

- Gold nanoparticles (BBI solutions) either 20, 40 or 60 nm
- ssDNA with -SH modification (DNA of choice, fluorescent DNA needed for quantification)
- Eppendorf vials (low binding preferred, not needed)
- 1 wt% Tween solution in MQ
- 5M NaCl solution in MQ
- 100 μ M stock mPEG solution in MQ of ~6kD mPEG (store in aluminum foil, max. use of 2 days in fridge (4°C -6°C))
- PBST (pH 7.4 and filtered with 0.01% Tween 20)
- Centrifuge
- Mercaptoethanol (for quantification)
- Plate reader (for quantification)

Steps:

Day 1

1. To 1000 μ l of AuNPs add 10 μ l of 1 wt% Tween 20 solution
2. Add desired concentration of 100 μ M mPEG (6kD) solution

Per 1000 μ l AuNPs:

μ M mPEG	0.002	0.1	0.2	1	5
μ l 100 μ M mPEG	0.02	1	2	10	50

3. Mix well and let stand for 20 minutes at room temperature

Add desired HS-DNA concentration

40 nm AuNPs, At OD = 1 (520 nm), # particles / ml = 9E10, surface area / 1 ml = 1.5E14 nm²

μ M DNA	0.01	0.1	0.2	1	5
μ l DNA (40 nm AuNPs)	0.1	1	2	10	50
nM DNA / cm ²	3.4	34	68	340	1710

20 nm AuNPs, At OD = 1 (520 nm), # particles / ml = 7E11, surface area / 1 ml = 2.9E14 nm²

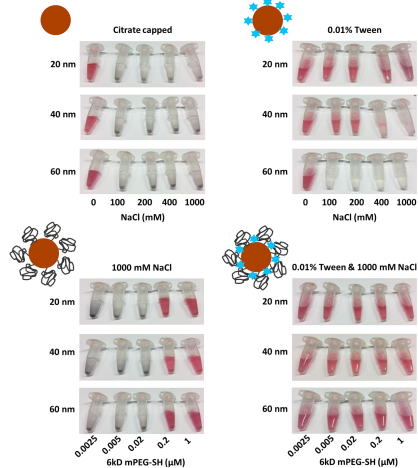
μ M DNA	0.005	0.05	0.1	0.5	1.5
μ l DNA (40 nm AuNPs)	0.194	1.94	3.889	19.4	97.2
nM DNA / cm ²	3.4	34	68	340	1710

Version: January 28th, 2021
Nienke van Dongen, BIOS lab on a chip group

Protocol conjugation of Gold Nanoparticles (GNPs) with ssDNA

Supplementary data

Effect of different addition steps of chemicals on the (salt) stability of AuNP of different sizes



Version: January 28th, 2021
Nienke van Dongen, BIOS lab on a chip group

5. Add 400 μ l 5M NaCl solution, mix well, and incubate for 1 hour

6. Centrifuge for 40 nm AuNPs 5 minutes at 4800 RCF, remove 800 μ l, add 800 μ l PBST, repeat for a total of 5-7 times; for 20 nm AuNPs 10 minutes centrifugation at 15000 RCF, remove 800 μ l, add 800 μ l PBST, repeat for a total of 5-7 times.

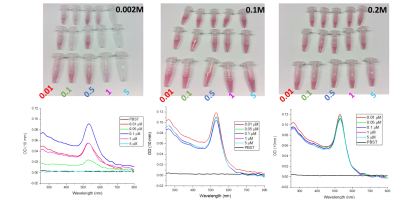
The AuNPs are now functionalized with DNA, you can store them in fridge (4°C -6°C) until further use. Some sedimentation can take place over time, this is no problem, just vortex before use.

! Do NOT store in THE FREEZER, this will cause aggregation of GNPs !

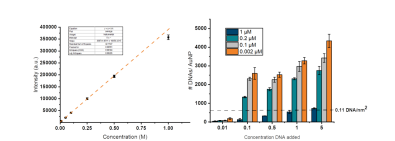
7. For quantification measure the OD at 520 nm at the nanodrop and use supplementary information to calculate the AuNP concentration
8. add 1.4 μ l of mercaptoethanol per 1000 μ l of AuNP solution, mix well and incubate overnight at room temperature
9. spin down at 4000 RCF for 10 minutes, take supernatant and measure fluorescence in the plate reader
10. compare to calibration curve of HS-DNA-fluo in the same well plate.

Version: January 28th, 2021
Nienke van Dongen, BIOS lab on a chip group

AuNPs after 1 hour incubation at room temperature



Quantification of DNA molecules on 40 nm AuNPs with different amounts of mPEG and different DNA concentrations



Determining AuNP concentration

The manufacturer (<https://www.bbi-solutions.com/>) supplies O.D. values for all samples. By plotting the known coefficients from literature over a dilution series of 40 nm AuNPs, a calibration curve was created for the concentration (M) related to the OD at 520 nm (at the nanodrop downstream (BIDS)).

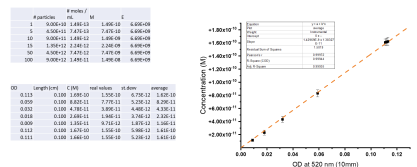


Figure 16: the original protocol, as adapted from Li et al. for use in this bachelorthesis.¹

10.2 Fluorescent DNA calibration

The four tables below illustrate the different volumes added in the eppendorf tubes. The different tubes are used to fill a microwell plate. This plate is added to a microplate reader, which in turn measures fluorescence in each well.

Tables 1 and 2 together illustrate the dilution series for the experiment without added mercaptoethanol. Tables 3 and 4 represent the second fluorescence calibration experiment. Based on the results of the first experiments, the second experiment includes lower concentrations. This was done because the fluorescence emitted by the lowest DNA concentration in the first experiment was detected by the microplate reader. This forced the second experiment to create lower concentrations, in hope of finding the L.O.Q and L.O.D.

Dilution number		a/b 1	a/b 2	a/b 3	a/b 4	a/b 5	a/b 6
PBS		760 μL	400 μL				
Volume, last used solution	40 μL	40 μL	100 μL	100 μL	100 μL	100 μL	100 μL
Concentration	100 μM	5 μM	1 μM	0,2 μM	0,04 μM	0,008 μM	0,0016 μM
Numerical concentration		$5 \cdot 10^{-6}$ M	$1 \cdot 10^{-6}$ M	$2 \cdot 10^{-7}$ M	$4 \cdot 10^{-8}$ M	$8 \cdot 10^{-9}$ M	$16 \cdot 10^{-10}$ M

Table 1: The first part of the dilution series. DNA is diluted in different steps. The first step uses stock PBS as a base. Following steps dilute a part of the previously used concentration. Part of the volume created in a/b 1 is transferred to be diluted further in a separate dilution curve.

Dilution number	1 alpha/beta	2 alpha/beta	3 alpha/beta	4 alpha/beta	5 alpha/beta	6 alpha/beta
PBS	250 μl	400 μL	400 μL	400 μL	400 μL	400 μL
Volume, last used solution	250 μl (from 1a or b)	100 μL				
concentration	2,5 μM	0,5 μM	0,1 μM	0,02 μM	0,004 μM	0,0008 μM
Numerical concentration	$2,5 \cdot 10^{-6}$ M	$5 \cdot 10^{-7}$ M	$1 \cdot 10^{-7}$ M	$2 \cdot 10^{-8}$ M	$4 \cdot 10^{-9}$ M	$8 \cdot 10^{-10}$ M

Table 2: The second part of the dilution series. The first volume is based on a/b 1 in the first dilution series.

Dilution number		a/b 1	a/b 2	a/b 3	a/b 4	a/b 5	a/b 6
PBS		792 µL	400 µL	400 µL	400 µL	400 µL	400 µL
Volume, last used solution	8 µL	8 µL	100 µL	100 µL	100 µL	100 µL	100 µL
Concentration	100 µM	1 µM	0,2 µM	0,04 µM	0,008 µM	0,0016 µM	0,00032 µM
Numerical concentration		1*10-6	2*10-7	4*10-8	8*10-9	1,6*10-9	3,2*10-10

Table 3: The first part of the dilution series with MCE. Notice that this table, and as such this part of the dilution series with MCE, is similar to the first experiment. The main difference is the starting concentration, which is lowered 5-fold in this setup.

Dilution number	1 alpha/beta	2 alpha/beta	3 alpha/beta	4 alpha/beta	5 alpha/beta	6 alpha/beta
PBS	250 µl	400 µL	400 µL	400 µL	400 µL	400 µL
Volume, last used solution	250 µl (from 1a or b)	100 µL				
concentration	0,5 µM	0,1 µM	0,02 µM	0,004 µM	0,0008 µM	0,00016 µM
Numerical concentration	5*10-7 M	1*10-7 M	2*10-8 M	4*10-9 M	8*10-10 M	1,6*10-10 M

Table 4: The second part of the dilution series with MCE. the first step in this series is based on step 1 in table 3, which is why there is more initial volume for this concentration.

10.3 Limit of detection for fluorescence

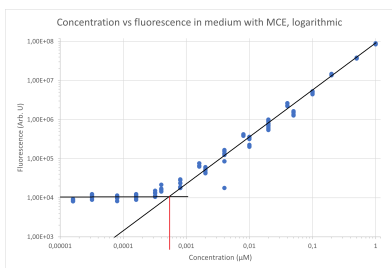


Figure 17: The L.O.D. found using the visual method.

As stated in the results and discussion, the L.O.D. has been found using two different methods. The first method visually finds the intercept between the linear part and the horizontal part of the curve. This can be seen in figure 17. The second method uses linear regression. It uses two formulas that use the standard deviation and slope to calculate the L.O.D. and L.O.Q. The formula for the L.O.D. is

$$\text{L.O.D.} = 3.3 * (\text{Standarddeviation}/\text{slope}) \quad (8)$$

while the formula for the L.O.Q. is

$$\text{L.O.Q.} = 10 * (\text{standarddeviation}/\text{slope}) \quad (9)$$

This is calculated using excel.

10.3.1 Comparison between fluorescence with and without MCE

In figure 18 a comparison between fluorescence with and without MCE was made. A linear fit was made to further illustrate the differences. In this figure only the results for concentrations of 0,32 nM and higher were used. This way the datapoints that are close to or below the L.O.D. are not a confounding factor for the linear fit. For both measurements the values for the negative controls have been removed. The highest concentration, 5 μ M, (measured in the dilution series without MCE) is included but is not shown in the graph.

There is a clear linear correlation between fluorescence intensity (in arbitrary units) and the concentration of fluorescent DNA, given here in μ M. The error bars show one standard deviation. With this data a formula can be created to relate fluorescence to the fluorophore concentration.

$$C = 1.46 * 10^{-8} * F - 4.46 * 10^{-3} \quad (10)$$

in which C is the a647n concentration and F is fluorescence (Arb. U). Which is strange; A647n shows higher fluorescence in the medium with added MCE than in pure PBS. this is unexpected as MCE is known to have a quenching effect on fluorophores. Additionally, the addition of MCE slightly lowers the concentration because of the added volume. This effect has not been compensated for. MCE has been known to alter fluorescence.³⁴ more research is needed to find out how MCE influences the fluorescence behaviour of a647n.

10.4 Gold nanoparticle stability

Experiment 2 was done in order to find which amount of mPEG needed to keep the AuNPs stable at high (1M+) salt concentrations. In order to find stability for 2 and 6 kDa mPEG a series has been made with different concentrations, ranging from 0.01 to 9 μ M. The kind of mPEG is not specified since both lengths are tested with the same conditions. table 5 shows the different amounts of mPEG and MilliQ added to 100 μ l of stock AuNP solution.

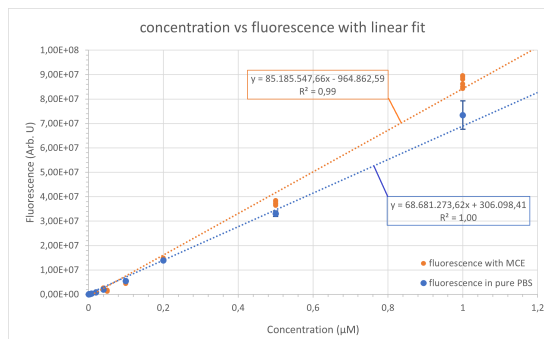


Figure 18: The calibration curve for the atto 647n fluorescent probe in PBS. All measurements have been done in triplicate, with an added technical duplicate. The error bars represent the standard deviation for all 6 measurements. For points without a visible error bar, the bars lie within the size of the data-point.

tube	1	2	3	4	5	6	7	8	9
μM mPEG	0,01	0,05	0,1	0,23	0,5	1	3	6	9
μL mPEG (1 μM)	1	5	10	23	-	-	-	-	-
μL mPEG (100 μM)	-	-	-	-	0,5	1	3	6	9
MilliQ	22	18	13	0	22,5	22	20	17	14

Table 5: A visualisation of the contents of the eppendorf tubes for each condition. As can be seen, 2 mPEG dilutions were made. This was done to keep the total added volume down, ensuring the difference between coagulated (transparent) and stable particles (red) is easy to determine.

10.5 Gold nanoparticle dilution series

In this section, the two tables for the two protocols are shown. The first table, table 6, gives the concentration range for the dilution curve for untreated AuNPs. The second table, table 7, shows the concentration range for the dilution curve made with mPEG & tween20 conjugated AuNPs. This table also shows a correction for the added volume due to the addition of said surface molecules. Lastly, in the results 530 nm is used to analyze the absorption. This choice will be substantiated in this section.

Dilution number	0	1	2	3	Dilution number	4	5	6	7	8
MilliQ	0 μl	80 μl	150 μl	450 μl	MilliQ	300 μl				
AuNP stock	300 μl	240 μl	150 μl	150 μl	Last used volume	200 μl				
Numerical concentration (M)	1,56 E-10	1,17 E-10	7,8 E-11	3,9 E-11	Numerical concentration (M)	1,56 E-11	6,24 E-12	2,5 E-12	9,99 E-13	3,99 E-13

Table 6: A visualisation of the dilution curve for AuNPs. This dilution series was made to dilute "pure" AuNPs. In other words: in this series only AuNPs are diluted in MilliQ, without any added surface molecules.

Dilution (linear)	1	2	3	4	logarithmic	5	6	7
PBST	0 μ l	50 μ l	100 μ l	300 μ l	PBST	300 μ l	300 μ l	300 μ l
Stock	200 μ l	150 μ l	100 μ l	100 μ l	Last used volume	100 μ l	100 μ l	100 μ l
Concentration (M)	1,56E-10	1,17E-10	7,8E-11	3,9E-11	Concentration (M)	9,75E-12	2,44E-12	6,09E-13
Concentration, corrected (M)	1,51E-10	1,13E-10	7,55E-11	3,77E-11	Concentration, corrected(M)	9,43E-12	2,36E-12	5,89E-13

Table 7: The dilutions for the AuNP calibration curve. The highest concentrations have a linear decrease, and at the lower concentrations, the curve switches to be logarithmic. This specific series corresponds with the dilution series for AuNPs with conjugated surface molecules. The concentration as stated is not entirely accurate because adding surface molecules also slightly increases the volume. Row 5 shows the corrected concentration.

As stated in the results, the dilution curves were made by taking the absorption at 530 nm. This value is presumed to be accurate to the highest absorption for 40 nm AuNPs. The microplate reader measured every wavelength between 400 and 800 nm, with steps of 5 nm. As can be seen in figure 19, the peak absorption lies around 530 nm for AuNPs coated with tween20 and 2kDa mPEG, and at the same value for AuNPs coated with tween20 and 6kDa mPEG. This absorption peak can also be found in the raw data, as can be seen in figure 20. The data constitutes the entire measured absorption spectrum for all measured wells. No distinction has been made between AuNPs coated with 2kDa and 6kDa mPEG in this figure. From left to right, the AuNP concentration in the wells decreases following the dilution series, with 6 wells for each condition. The light gray area at the right hand side are spectra taken from wells containing just PBS. The dark gray area consists of stock AuNP colloid.

The highest absorption for each well is coloured green. As can be seen, for the highest AuNP concentrations, the peak lies at 530 nm. Although, at lower concentrations, another peak becomes more prominent. This is the peak at 400 nm. In figure 19, this high point can also be seen, although the measurements cut off at this wavelength. In order to remove uncertainty about which peak is measured, just measuring at 530 nm was chosen to be optimal. An extra confirmation was done by measuring if there was a local peak. This maximum value was measured between 470 and 590 nm. These values are less exact, and as such should be taken less into account.

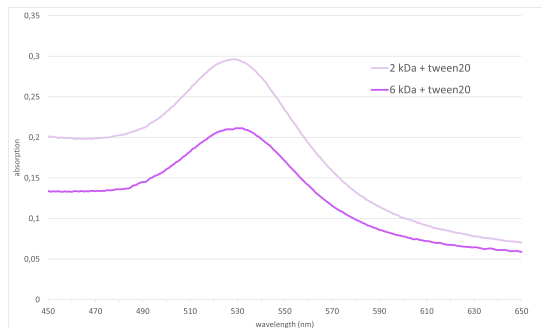


Figure 19: Absorption spectra for AuNPs coated with 2kDa mPEG & tween20 and 6kDa & tween20. Peak intensity difference is due to error in the measuring method since the calibration curves do not show such a large difference.

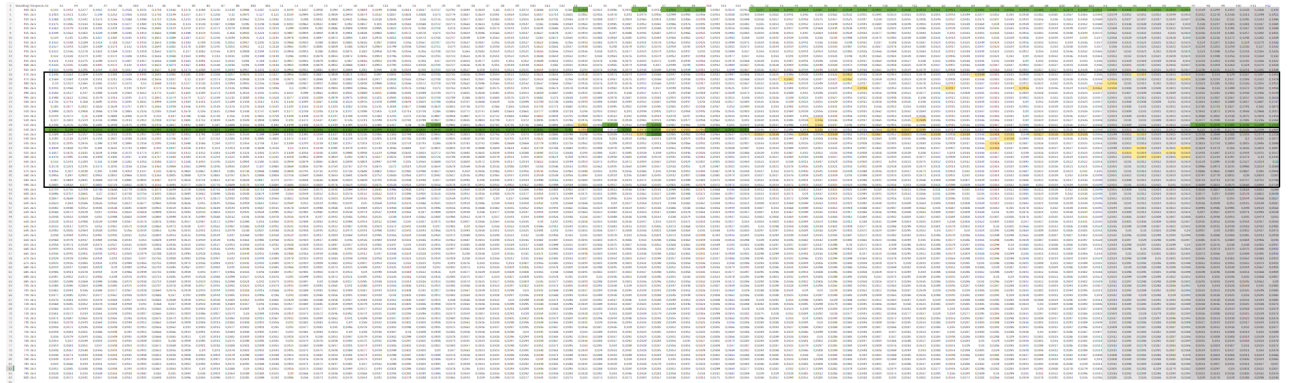


Figure 20: All data collected for the measurement of AuNPs with added mPEG. A blanco mmeasurement (light gray) and pure AuNPs(gray) are also included. Furthermore, peaks are analysed within the entire spectrum for each value (green), and within a 60 nm range from 530 nm (both shown with black borders around the cells).

To conclude: the raw data shows that there is a clear peak at 530 nm for coated AuNP. mPEG does not influence the wavelength at which there is peak absorption. For non-coated AuNPs this absorption peak lies at 525 nm. This corresponds with the data provided by the supplier²¹. At or below a wavelength of 400 nm, there is a second peak. For consistency, measuring at 530 nm is the best course of action.

10.6 HS-DNA loading on AuNPs

For DNA loading on the AuNPs different DNA concentrations were used. This can be seen in table 8

Strands/np, theoretical no restrictions	500	2500	50000	100000
μl DNA per 1200 μl AuNPs (or per 400 μl with 3 times higher concentration)	0,94	4,69	9,37	18,74
DNA max strands per well (100 μl)	1,415E+13	7,0610+13	1,4107E+14	2,8214E+14

Table 8: the HS-DNA concentrations added to the 2kDa and 6kDa + tween20 functionalised AuNPs.

10.7 target DNA loading

To determine target DNA loading the same concentrations were used to conjugate HS-DNA. For target DNA loading a 100* excess was used with respect to the highest found concentration of HS-DNA on the AuNPs

10.7.1 washing steps calculation

this section shows the washing steps done in experiment 5. As these calculations show, the concentration of free floating DNA in the wells is below the L.O.D.

Target DNA washing steps calculations

Diluting DNA

17,98 μl , 100 μM target DNA added to \pm 1000 μl solution

$$\frac{100 * 10^{-6} * 17,98 * 10^{-6}}{1017,98 * 10^{-6}} = 1,766... * 10^{-6} M = 1,798 * 10^{-9} \text{ mole}$$

$$1,798 * 10^{-9} * \text{Constant of avogadro} = 1,08... * 10^{15} \text{ strands added}$$

Washing steps

Every step 800 μl gets replaced.

$$\frac{1018 \mu\text{l} - 800 \mu\text{l}}{1018 \mu\text{l}} = 0.214...$$

Every washing step the concentration is 0.214... * the previous concentration.

This is done a total of 7 times.

$$1,08... * 10^{15} * 0,214...^7 = 2,23... * 10^{10} \text{ strands total}$$

Taking volume for in the wells

Every well contains 100 μl

$$2,236... * 10^{10} * \frac{100}{1018} = 2,196... * 10^9 \text{ strands per well}$$

Which corresponds with $3,647 * 10^{-15}$ mole, or $3,647 * 10^{-11} M$ which is about 2 orders of magnitude smaller than the L.O.D. found using linear regression

Figure 21: A series of calculations showing the washing steps should produce a concentration of DNA in the wells two orders of magnitude below the L.O.D. This means any detected fluorescence cannot be due to free floating DNA.

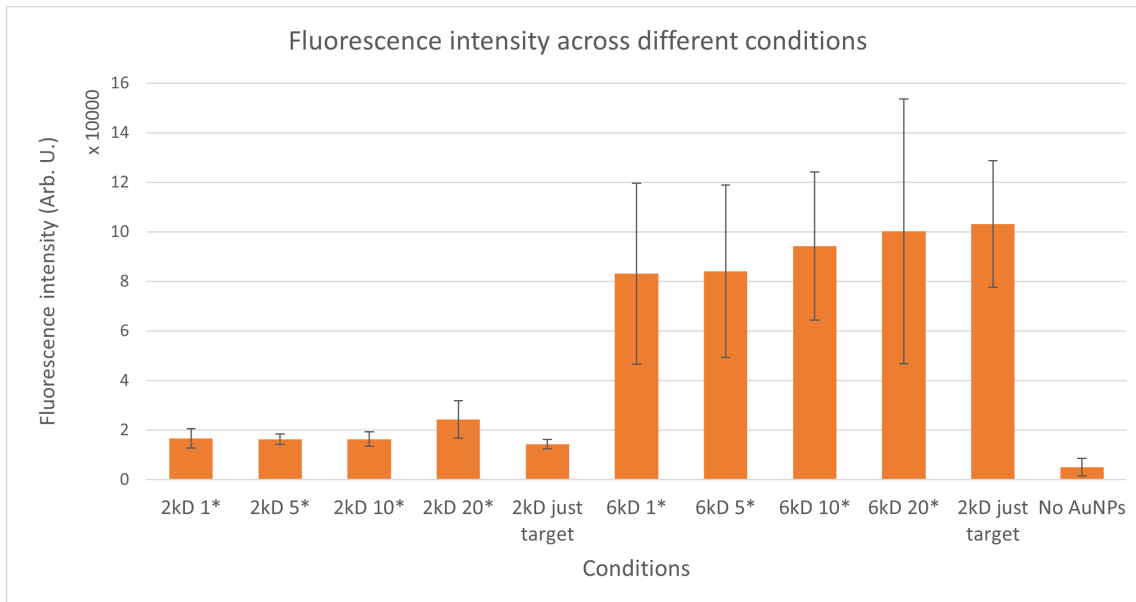


Figure 22: Different fluorescence values for A647n, from left to right, different HS-DNA conditions on 2kDa mPEGylated AuNPs, a measurement without added HS-DNA, different HS-DNA conditions on 6kDa mPEGylated AuNPs, a measurement without added HS-DNA, and the blanco measurements

10.7.2 Fluorescence comparison, target DNA, unbound target DNA and blancos

When measuring target DNA fluorescence, the results showed to be well below the limit of quantification but above the limit of detection. To show there is indeed a noticeable difference in fluorescence, figure 22 was constructed. Fluorescence is shown for all conditions. Additionally, a blanco measurement was added. The wells used in these measurements only contain PBS and MCE. No other molecules were added

10.8 additional information

The specific protocols used in this thesis are available on request. Please contact the author to gain full access.